WTC 2005 Year End Update

Christopher W. Lum*

December 22, 2005

Introduction

Maritime search and surveillance-type missions typically require heavy human involvement. A set of unmanned aerial vehicles (UAVs) has the potential to provide a "sensor network" to greatly increase efficiency and effectiveness of these surveillance type missions. However, limited autonomy is still a bottleneck to networked UAV applications. High operator involvement is required in logistics and operation, for example, distributing assignments such as which regions to search and coordinating subsequent sensor measurements. In a noisy environment, it becomes difficult for a human operator to classify sensor readings and assign confidence in these readings. Determining regions of high target-location probability and coordinating nearby agents to converge on a particular spot while allowing other vehicles to continue searching is also difficult. Therefore, the primary limitation to concurrent operation of multiple vehicles remains lack of autonomy of these vehicles.

The current work aims to develop target identification and searching algorithms for the Georanger UAV [1] for aero-magnetic surveying. A specific application is the detection of a submarine in littoral waters based on its magnetic signature. Eventually, these algorithms would be developed to operate with a team of heterogeneous vehicles. This team would be comprised of individual vehicles known as agents. Each agent could have different capabilities and sensors which dictates that algorithms be easily adaptable to accommodate these differences.

A summary of the completed, current, and future research activities with this project include:

Completed Research

- Creation of task and path-planning control architecture.
- Preliminary system and sensor (magnetometer) modeling for simulations.

*Research Assistant, Department of Aeronautics and Astronautics, email: lum@aa.washington.edu

- Integration of high fidelity total magnetic intensity (TMI) maps from Fugro Airborne Surveys.
- Development of target identification using particle filter state estimation technique.
- Development of simple occupancy map based searching algorithm for heterogeneous teams of agents.

Current Research

- Refinement of searching algorithm using model predictive control techniques.
- Implementation of simulation on high fidelity hardware-in-the-loop (HiL) simulator using embedded processor running INTEGRITY real time operating system.

Future Research

- Analysis of communications relay logic between multiple Georangers and one or more ground stations.
- Integration of searching and target identification algorithms into the task and path-planning architecture [2].
- Distributed simulation heterogeneous team of agents using distributed test-bed.
- Flight test of algorithms using Insitu GeoRangers and/or ScanEagles.

1 Completed Research

1.1 Task and Path-Planning Architecture

In the simplest form, the task and path-planning architecture can be visualized in a block diagram as shown in Figure 1.

The inner loop controller (also known as the autopilot) is assumed to be provided. The target identification and searching algorithms that are being developed reside on the guidance controller. Section 3 contains more discussion regarding its development and the hardware-in-the-loop simulation.

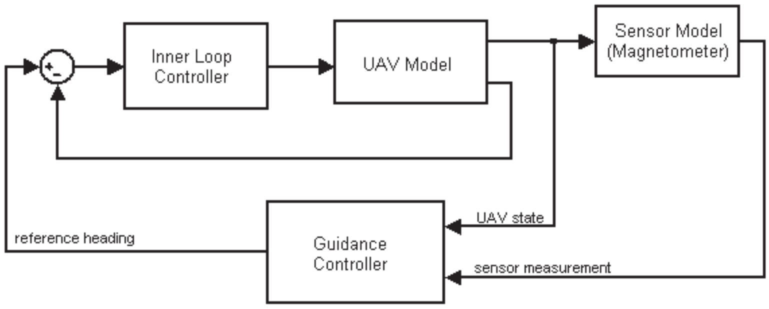

Figure 1: Block diagram of task and path-planning architecture

1.2 Total Magnetic Intensity Maps

When an actual search is executed, differences between the ground station map of the magnetic field and the actual magnetic field will appear as magnetic anomalies. In this work, to minimize the number of false anomaly encounters and to increase the accuracy of the evaluation, actual magnetic survey data is used as a local TMI map. This data is provided by Fugro Airborne Surveys. The data was collected by a manned aircraft equipped with a magnetometer to measure the TMI. This information, coupled with a GPS position, provides the TMI in "line data" form. This data can then be interpolated into a 100x100 meter grid. TMI readings at locations other than survey points are linearly interpolated from this grid. A magnetic map of a region in the Gulf of Mexico and a simple grid search trajectory are shown below in Figure 2(a). Here, the data is acquired in an approximate 60x50 km grid. The regions of uniform color denote areas where survey data is not available, creating the "staircase" appearance. Assuming that there are only permanent fixtures in the region when the map is acquired, this map now makes up the reference set of data on the ground station.

In addition to a local magnetic map, a magnetic model of the desired target is also required. In the following example, the magnetic signature of the target (an idealized submarine) is modeled as a simple two dimensional Gaussian distribution, shown in Figure 3. The magnetic signature of the target is a function of many variables, namely depth of target, sensor altitude, etc. For current purposes, the target is assumed stationary and at a fixed depth, thereby rendering the magnetic signature static. Assuming that the magnetic signature of the target simply adds to the total magnetic intensity of the local region in a linear fashion, anomalies can easily be identified by simply subtracting the magnetometer reading from the local reference map which is stored on the ground station.

The described approach can be used to compare magnetometer readings with the reference data to create a differential measurement. Large differential measurements imply the presence of a new magnetic anomaly and possible target. If the agent does not fly over any targets, the magnetic anomaly should

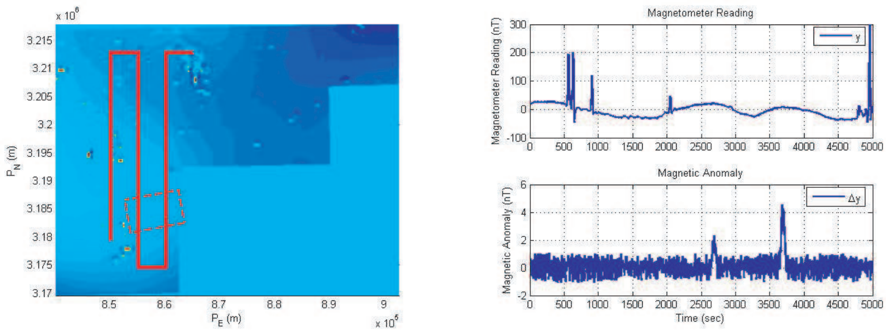

(a) Total magnetic intensity map.
(b) Associated magnetic traces.

Figure 2: The total magnetic intensity map and trajectory over area with corresponding magnetometer readings.

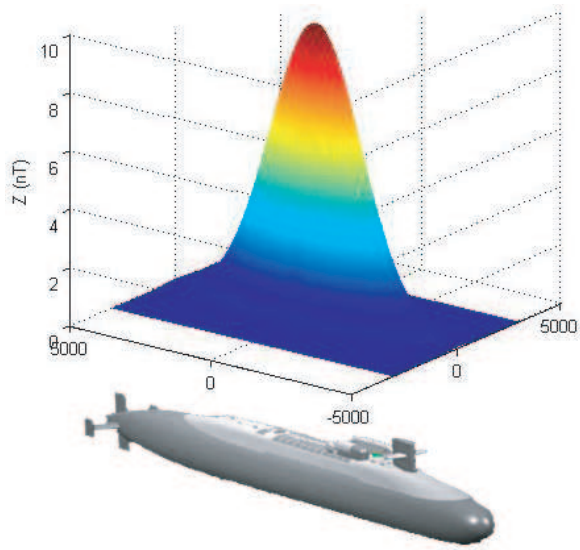

Figure 3: Magnetic signature of target. Magnetic signature given by $z = h(x, y)$.

be near zero. Small non-zero anomaly encounters can be attributed to temporal variations in magnetic field and sensor noise. A simple grid search pattern was shown previously in Figure 2(a). The location of the target is shown as a dashed red box and the trajectory of the agent is shown in the solid red line (starting in the lower left corner). The associated total magnetic intensity trace and differential measurement trace is shown in Figure 2(b). The total magnetic intensity reading as the agent flies over this trajectory is shown in the upper trace and the differential measurement is shown in the lower trace. As the agent flies this search trajectory, the sensor measurement is constantly compared to the reference data set to generate a differential measurement. As can be seen in Figure 2(b), given the differential magnetometer reading, it is obvious how to detect where the anomaly occurred (two spikes at approximately 2700 and 3700 seconds) even though the actual range of absolute measurements may be large.

1.3 Target Identification

Magnetic anomalies can be caused by many factors such as temporal variations in the magnetic field or false targets encounters (i.e. boats/vessels). Once a magnetic anomaly is encountered, it must be identified and classified. On simplistic level, the overall goal is to either classify the anomaly as the desired target or a false reading. Obviously, it would be simple to identify the anomaly if the entire magnetic signature of the anomaly is obtained (the UAV flies over the entire boxed region in Figure 2(a)). However, this requires many passes over a potential target, and significant time to make the necessary measurements. If the anomaly is moving or evading, this may not be feasible. The question now becomes, given only one or two passes over the target, is it possible to correctly identify or provide a probability that this anomaly is indeed the target being sought after? To address this issue, a particle filter method is used [3].

A particle filter is a recursive, non-parametric Bayes filter technique which estimates the states of a system using a finite number of state hypotheses [4].

GPS allows the position of the agent in the earth frame to be computed, but the target location and orientation in the earth frame is not known. The goal of the particle filter is to estimate the state of the agent (position and orientation with respect to the target, expressed in the target's frame of reference).

When an agent encounters an anomaly whose magnitude exceeds the noise threshold (approximately 1 nT in this case), the particle filter is started in an attempt to estimate the state of the agent with respect to the target. The particle filter's progression as the agent flies diagonally over the target is displayed over a top down view of the target signature (Figure 3) and is shown below in Figure 4.

In this sequence, the large red circle represents the actual location of the agent and the solid red line represents the agent's trajectory over the target. The smaller purple dots represent the particle filter's many different hypotheses of the possible state of the agent (position north, position east, and heading). The actual agent crosses over the target starting in the lower left corner and flies over it to the upper right corner.

As the agent obtains more and more sensor measurements (at a simulated rate of 1 Hz), the particle filter is able to eliminate particles which are inconsistent with the current measurement and resample these particles to regions which have a higher probability of producing the actual sensor reading. This is why as time progresses, the particles become concentrated around the actual UAV location. Near the end of the simulation, there are four distinct groups of particles. This is due to the symmetry of the underlying target signature. Each

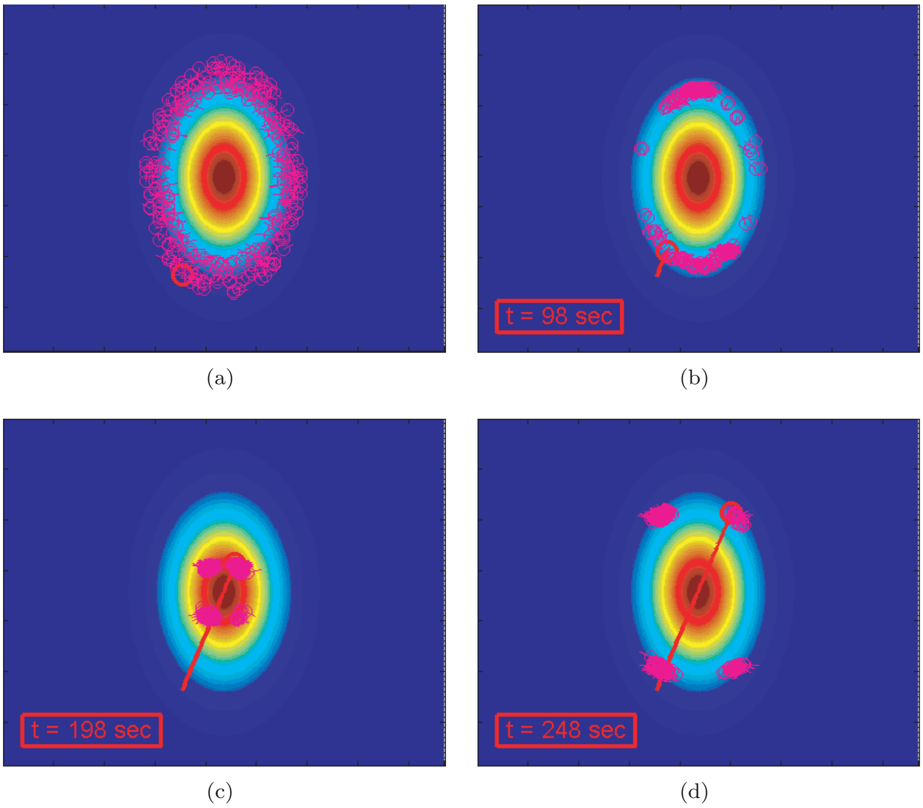

(a) (b) (c) (d)

Figure 4: Particle filter progression during a target encounter. The solid line indicates actual aircraft position relative to target signature, while the particles concentrate about possible positions

of these four groups of particles are equally likely because each group would produce the correct actual sensor readings.

A quantitative measure of the particle filter's confidence for an encounter with the actual target and an encounter with a false anomaly is shown below in Figure 5.

In Figure 5, the difference between a true target encounter and a false anomaly encounter is fairly clear. In the situation where the agent encounters the true target, the confidence measure increases initially as the particles are quickly resampled to locations which are consistent with the actual sensor measurements and then stays fairly constant. However, in the case where the agent encounters a false anomaly, the particle filter regularly "loses confidence" as inconsistent sensor measurements are obtained. This is characterized by the sharp drops in the sum of the particle weights. Current research is directed towards training a neural net to recognize these features and thus provide a qualitative measure to the target identification problem. In the end, the parti-

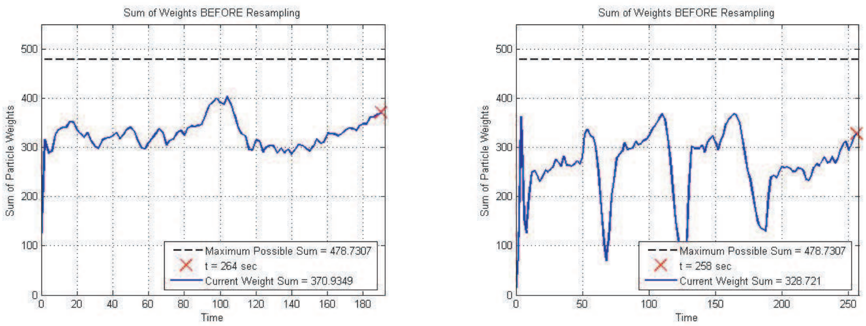

(a) True target encounter

(b) False anomaly encounter

Figure 5: Sum of all particle weights during a true target encounter and a false anomaly encounter.

cle filter will provide the trace of the sum of the weights over time (Figure 5) and the neural net will process this trace. In combination, the particle filter and neural network provide a mapping from magnetic sensor measurements to a single scalar value which represents a measure of how confident the particle filter is that the encountered anomaly is the desired target or not.

1.4 Simple Team Searching

The particle filter method is used to identify anomalies once they are encountered. A method to actively search for targets and anomalies is now considered.

As can be seen in Figure 2(a), one search pattern that can be used is a simple grid search pattern. However, for a team of autonomous agents, a more intelligent approach is desirable. In this situation, an occupancy based map search is employed. In this scheme, the search domain is discretized into rectangular cells. Each cell is assigned a score based on the probability that the target is located in that grid. This is similar to a two dimensional, discretized probability density function [5]. This centralized occupancy based map is shared and updated by all agents involved in the search. At each time step, guidance decisions for each agent are chosen based on this map. Controls for each agent are chosen based on maximization of a team utility function.

Once the controls for each agent are assigned, it becomes necessary to update the score of each cell based on the agent's findings. As an agent finishes searching a cell, if no anomaly is discovered, the score of the cell can be updated using the sensor model for each agent. In the event of an anomaly encounter, the particle filter is used to identify and classify the anomaly. If it is determined that it is not the target, a low score is assigned to that cell. If the anomaly is determined to be the target, then the surrounding cells of the occupancy map within a certain radius have their scores increased. The radius chosen can be a function of the target identification algorithm's confidence that the anomaly is indeed the target. This allows for a local increase in belief of the target position while leaving other areas unaffected.

The formulation of the utility function and the occupancy map update also caters to the theme of heterogeneity that was introduced with the particle filter. Both the utility function and occupancy map update equation can be adjusted to accommodate for a heterogeneous team of agents.

In the following example, a simple two dimensional Gaussian distribution is used to increase the scores over the two dimensional space where the target is located. A search with three agents is shown below in Figure 6.

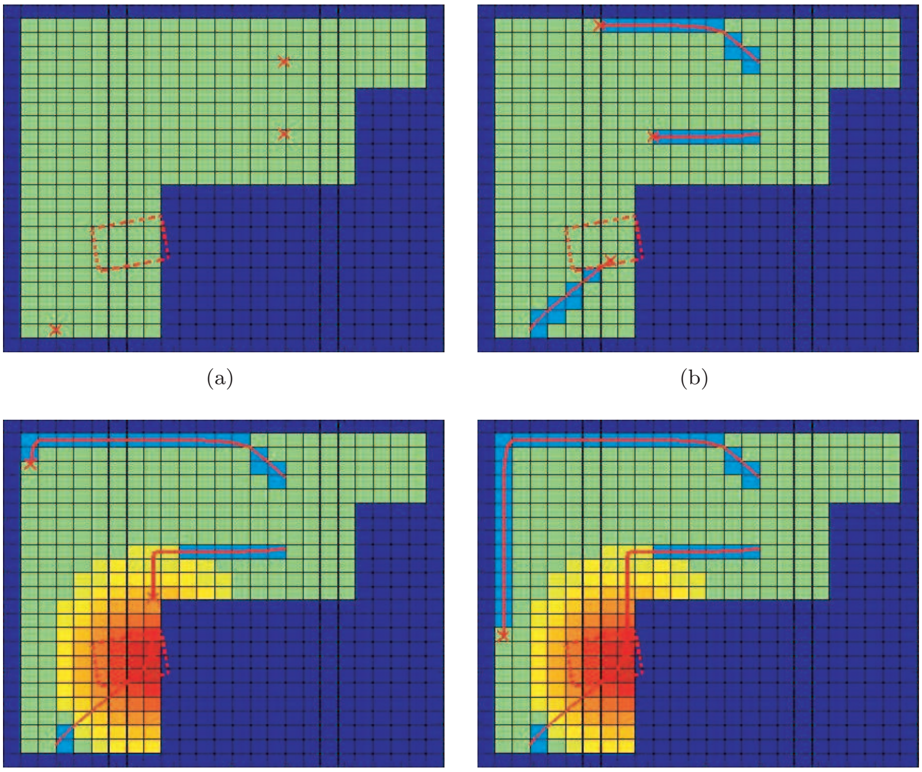

(a) (b) (c) (d)

Figure 6: Occupancy based map search with three agents.

In this situation, the target location is shown as the dashed, red box and the agents are represented by red x's. Figure 6(a) shows the initial location of the agents relative to the target. In Figure 6(b), one of the agents is about to encounter an anomaly. In this case, the anomaly happens to be the target and therefore, the particle filter is able to identify and classify this anomaly as the target and the agent makes a positive ID at its current cell. This then updates the nearby occupancy map cells with increased scores. This causes the second agent to converge and investigate this location as shown in Figure 6(c).

However, the third agent continues searching the other regions of the map as seen in Figure 6(d).

2 Current Research

2.1 Refinement of Team Based Searching Algorithms

The current searching algorithm is based on updating a central occupancy map and maximizing a team utility function. However, the utility function is somewhat simple and is limited in its predictive capabilities. Current research is directed at formulating this as a model predictive control problem and employ evolutionary computational methods to optimize the associated utility function [6].

Another improvement is to implement patrol regions for each agent based on its individual capabilities. These patrol regions could still overlap and would dictate which possible trajectories are feasible at each generation of the evolutionary computation process. The look-ahead horizon could be extended as far as would be computationally efficient given the number of agents and the complexity of the team based utility function. This idea is illustrated below in Figure 7.

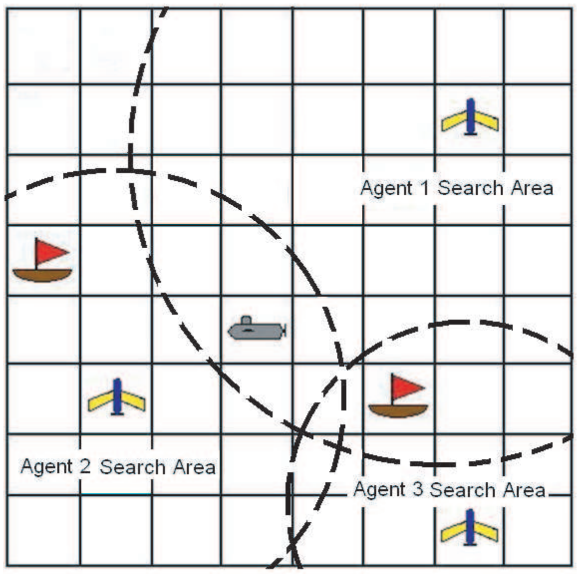

Figure 7: Multi agent team with individual patrol areas.

2.2 Hardware-in-the-Loop Simulation

Once the numerical simulation is complete, the next step in this process is to run this simulation using a hardware-in-the-loop (HiL) simulator of the ScanEagle UAV. This involves programming the searching algorithms as embedded applications on an Embedded Planet 8260 single board computer (shown in Figure 8(a)). Current research efforts are directed towards developing real time embedded applications using the INTEGRITY operating system. Once these applications are created, the searching and other guidance algorithms will be able to interface with the HiL simulator (Figure 8(b)). In addition to simply porting the current algorithms to the new operating system, a library of interface functions must be developed in order to allow for communication of data packets between the inner loop (autopilot) and outer loop (guidance controller).

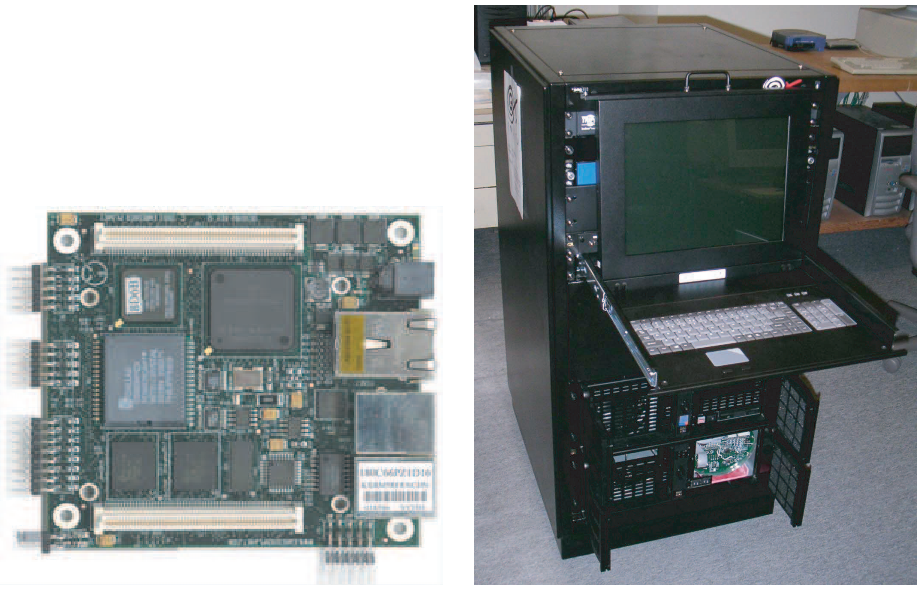

(a) EP8260 single board computer (b) SeaScan HiL simulator

Figure 8: Embedded hardware used for HiL simulation

3 Future Research

3.1 Distributed Simulation

The HiL simulator shown previously is capable of providing a high fidelity plant model for a single agent. In the future, as the algorithms become more refined, it becomes necessary to provide a networked simulation with several high fidelity models. In addition to the dynamics of each model, the communication between agents must also be tested. An architecture for simulating the dynamics and communication between multiple agents is shown below in Figure 9.

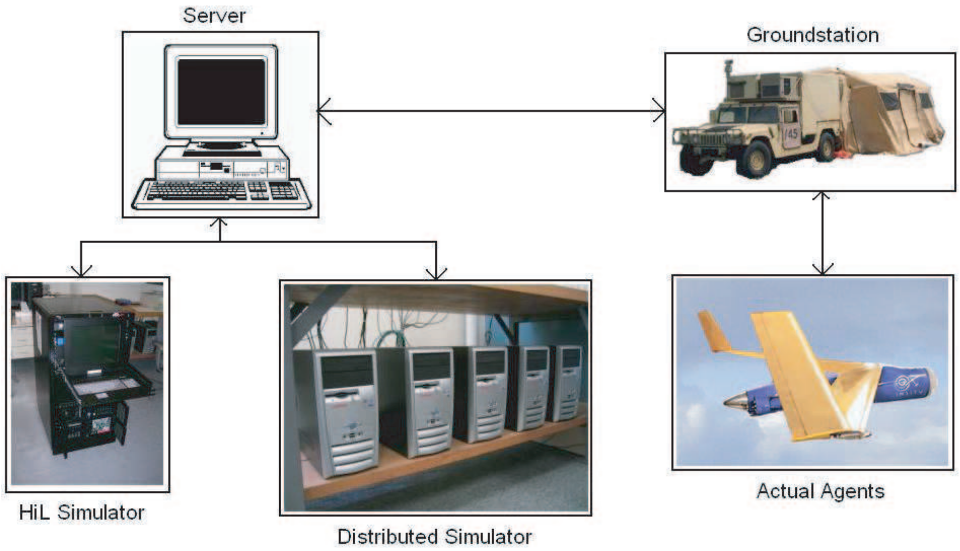

Figure 9: Distributed architecture for simulation and testing of a multi-agent team

In this setup, several high fidelity plant models can be simulated using the Distributed Test-bed available to us at the Autonomous Flight Systems Laboratory. The Distributed Simulation Test Bed consists of five simulation computers running simulation software. It is meant to be a high fidelity testing environment in that it accurately simulates the timing and data transfer required for the cooperative planning algorithms. This system could operate in parallel with both the HiL simulator and actual agents in field. This would allow for simulation and testing of nearly all aspects of this system including heterogeneous teams, dynamics, and communications.

3.2 Flight Tests

Finally, we hope to be able to one day apply these guidance algorithms to the actual Georanger and/or SeaScan UAVs and fly actual test missions. This would be a true testament to the potential of these ideas and a way to show that they have real-world applications and viability.

References

[1] "The Insitu Group," GeoRanger UAV Specifications, `http://www.insitugroup.com/prod_georanger.cfm`.

Figure 10: Georanger UAV produced by the Insitu Group.

[2] Pongpunwattana, A. and Rysdyk, R., "Real-Time Planning for Multiple Autonomous Vehicles in Dynamic Uncertain Environments," *AIAA JACIC*, December 2004, pp. 580–604.

[3] Lum, C. W., Rysdyk, R. T., and Pongpunwattana, A., "Autonomous Airborne Geomagnetic Surveying and Target Identification," *Proceedings of the 2005 Infotech@Aerospace Conference*, Autonomous Flight Systems Laboratory, Arlington, VA, September 2005.

[4] Thrun, S., Burgard, W., and Fox, D., *Probabilistic Robotics*, MIT Press, 2005.

[5] Bourgault, F. and Durrant-Whyte, H. F., "Communication in General Decentralized Filters and the Coordinated Search Strategy," *Proceedings of the 7th International Conference on Information Fusion*, Australian Centre for Field Robotics, Stockholm, Sweden, 2004.

[6] Pongpunwattana, A., *Real-Time Planning for Teams of Autonomous Vehicles in Dynamic Uncertain Environments*, Ph.D. thesis, University of Washington, Seattle, WA, June 2004.